

1 **Plasticity of the dopaminergic phenotype and of locomotion in**
2 **larval zebrafish induced by changes in brain excitability during**
3 **the embryonic period.**

4
5 *Embryonic excitability modulates differentiation*

6 Sandrine Bataille*¹, Hadrien Jalaber*¹, Ingrid Colin*¹, Damien Remy¹, Pierre Affaticati²,
7 Cynthia Froc¹, Philippe Vernier¹ and Michaël Demarque**¹.

8 1. Paris Saclay Institute of Neuroscience, (UMR9197) CNRS and Université Paris-
9 Saclay; Avenue de la Terrasse, 91190 Gif-sur-Yvette, France

10 2. TEFOR Paris-Saclay, CNRS UMS2010 / INRAE UMS1451, Université Paris-Saclay,
11 Avenue de la Terrasse, 91190 Gif-sur-Yvette, France

12 *authors contributed equally; **Corresponding author

13 ∴ *Corresponding author email address: michael.demarque@cnr.fr*

14 ∴ *Number of pages: 38*

15 ∴ *Number of figures, tables, multimedia, and 3D models (separately): 6/0/0/0*

16 ∴ *Number of words for abstract, introduction, and discussion: 228/646/1257*

17 ∴ *Acknowledgments:* The authors thank Kei Yamamoto for scientific inputs, TEFOR
18 Paris Saclay (TPS) for technical support.

19 ∴ *Conflict of interest statement:* The authors declare no competing financial interests.

20 ∴ *Funding sources:* This work was funded by the French National Research Agency
21 (ANR project “PallEnody”) and the Fondation pour la Médicale Recherche, FRM (“team
22 FRM”).

23 **Abstract (228/250 w):**

24 Neuronal communication starts before the establishment of the synapses with forms
25 of neuronal excitability occurring during the embryonic period, we called here
26 Embryonic Neuronal Excitability (ENE). ENE has been shown to modulate the correct
27 unfolding of development transcriptional programs but the global consequences for
28 the developing organisms are not all understood. Here we monitored calcium
29 transients as a proxy for ENE in zebrafish to assess the efficacy of transient
30 pharmacological treatments applied by balneation during the embryonic period to
31 modulate ENE. We also report lasting effects of 24h treatments, performed at the end
32 of the embryonic development, on morphology and behavior of larval zebrafish.

33 The post-mitotic differentiation of the dopaminergic phenotype is modulated by ENE
34 in the forebrain. The plasticity of the dopaminergic specification occurs within a stable
35 population of vMAT2 immuno-reactive cells, hence identifying an unanticipated
36 biological marker for this reserve pool.

37 We also report an effect of ENE on locomotion several days after the end of the
38 treatments. In particular, the increase of ENE from 2 to 3 dpf promoted an
39 hyperlocomotion in 6dpf zebrafish larvæ which is an endophenotype for Attention
40 Deficit with Hyperactivity Disorders and schizophrenia in zebrafish. These results
41 provide a convenient framework to identify environmental factors that could regulate
42 ENE and to study further the molecular mechanisms linking ENE to the
43 neurotransmitters specification, with clinical relevance for the pathogenesis of
44 neurodevelopmental disorders.

45

46 **Significance Statement (106/ 120 w):**

47 - Spontaneous calcium spikes, used as a proxy for Embryonic Neuronal Excitability
48 (ENE), are detected in the forebrain of embryonic zebrafish.

49 - Transients pharmacological treatments applied by balneation could be used to
50 increase or decrease ENE.

51 - The post-mitotic differentiation of the dopaminergic phenotype is modulated by ENE
52 in the zebrafish forebrain.

53 - The plasticity of the dopaminergic specification occurs within a reserve pool of
54 vMAT2 immuno-reactive cells.

55 - Transient increase of ENE at the end of the embryonic period induces a
56 hyperlocomotion, a phenotype associated with ADHD and schizophrenia in this model.

57 - Our results open clinically relevant perspectives to study the pathogenesis of
58 neurodevelopmental disorders in zebrafish.

59 **Introduction (646/750 w)**

60 During brain development, specific molecular components of the synaptic neuronal
61 communication such as ion channels, neurotransmitters and neurotransmitter
62 receptors are expressed and functional before synapse formation (Spitzer et al., 2002).
63 They contribute to immature forms of cellular excitability and intercellular
64 communications we propose to refer to as Embryonic Neuronal Excitability (ENE).
65 There is for instance a paracrine communication mediated by activation of receptors
66 by endogenous neurotransmitters, GABA and glutamate, in the neonatal rat
67 hippocampus, or glycine in the mouse spinal cord (Demarque et al., 2002; Owens &
68 Kriegstein, 2002; Scain et al., 2010). Acute changes of calcium concentration have
69 also been described, including filopodial or growth cone transients, and calcium spikes

70 in differentiating neurons (Gomez & Spitzer, 1999; Gomez et al., 2001; Borodinsky et
71 al., 2004). Calcium spikes are sporadic, long lasting global increase of intracellular
72 concentration of Ca^{2+} that occurs during restricted developmental windows called
73 “critical periods”. They have been identified in the developing brain of several
74 vertebrate species (Owens & Kriegstein, 1998; Borodinsky et al., 2004; Crepel et al.,
75 2007; Blankenship & Feller, 2010; Demarque & Spitzer, 2010; Warp et al., 2012;
76 Plazas et al., 2013). Quantification of calcium spikes by calcium imaging can be used
77 as proxy for ENE. Changes in the incidence and frequency of calcium spikes modulate
78 the specification of the neurotransmitter phenotype in neurons, as it is the case for
79 dopamine (DA), in several cell populations of the xenopus and mouse brain, with
80 consequences on several behaviors (Dulcis & Spitzer, 2008; Dulcis et al., 2013, 2017).

81 DA is an evolutionary conserved monoamine involved in the neuromodulation of
82 numerous brain functions in vertebrates, including motivational processes, executive
83 functions and motor control (Klein et al., 2019). Accordingly, alterations of the
84 differentiation and function of the neurons synthesizing DA contribute to the
85 pathogenesis of several brain disease with a neurodevelopmental origin, such as
86 Attention Deficit Hyperactivity Disorder (ADHD) and schizophrenia (SZ)(Lange et al.,
87 2012; Murray et al., 2017).

88 Further addressing the complex molecular and cellular mechanisms linking
89 developmental excitability, dopaminergic differentiation and behavioral outputs
90 requires an *in vivo* approach in a model accessible, genetically amenable and with
91 possible parallels with the human situations. The developing zebrafish *Brachydanio*
92 *rerio* fits with these needs. The development of the embryos is external, which allows
93 inducing perturbations of ENE at stages that would be *in utero* in mammalian models.
94 The embryos are relatively small and transparent, simplifying high-resolution imaging

95 of the brain in live or fixed preparations. Despite difference in the brain organization,
96 notably a pallium very different from the 6-layered cortex of mammals, the main
97 neuronal systems of vertebrates are present in zebrafish and respond to psychoactive
98 drugs (Gawel et al., 2019). In addition, the monoaminergic system has been
99 extensively studied in zebrafish (Schweitzer & Driever, 2009; Schweitzer et al., 2012).
100 In vertebrates, DA modulates executive functions, such as working memory and
101 decision making, through innervation of specific regions of the telencephalon. In the
102 zebrafish brain, most DA neurons innervating the telencephalon have their cell bodies
103 located within the telencephalon itself (TelDA cells)(Tay et al., 2011; Yamamoto et al.,
104 2011). To the best of our knowledge, there is no evidence for a plasticity of the
105 neurotransmitter phenotype in these cells.

106 To perturb ENE in conditions close to physiological exposure and ecotoxicology,
107 we used pharmacological treatments by balneation from 48 to 72 hours post
108 fertilization (hpf). We then analyzed the consequences of these transient
109 pharmacological treatments a few days later, between 6 and 7 days post-fertilization
110 (dpf). We report quantifiable changes in the specification of the dopaminergic
111 phenotype in TelDA neurons. We also report changes for high-speed swimming
112 episodes. These results suggest a role of ENE on the specification of the dopaminergic
113 phenotype and motor control in the zebrafish. They also open important perspectives
114 for this model to decipher the chain of events leading from environmental factors to the
115 pathogenesis of disorders such as schizophrenia and ADHD.

116 **Materials and Methods**

117 **Fish strains**

118 All experiments were carried out in accordance with animal care guidelines
119 provided by the French ethical committee and under the supervision of authorized
120 investigators.

121 Zebrafish were raised according to standards procedures. Briefly, for breeding,
122 males and females zebrafish were placed overnight, in different compartments of a
123 tank with a grid at the bottom that allows the eggs to fall through. The next morning the
124 separation was removed and after few minutes, the eggs were collected, rinsed and
125 placed in a petri dish containing embryo medium (EM). Embryos were kept at 28
126 degrees, then staged as hours post fertilization (hpf) according to specific criteria. The
127 number of animal used for each experiments is indicated in the corresponding figure
128 legends.

129 **Pharmacological treatments**

130 Pharmacological compound, veratridine (10 μ M), TTX (2 μ M), ω conotoxin (0.08
131 μ M), nifedipine (0.4 μ M) and flunarizine (2 μ M) were purchased form R&D System (UK)
132 and prepared in water except veratridine which required dimethyl sulfoxide (DMSO) for
133 dissolution and flunarizine that requires ethanol for dissolution. Sham control were
134 performed using the same concentration of DMSO in EM without the drug to rule out
135 an effect of the detergent itself. Specific period and duration of applications are
136 indicated in the corresponding figure legends. All pharmacological treatments were
137 performed by balneation followed by three washes in EM. Embryos were randomly
138 distributed in wells (30 embryos per well) of a 6-well plate containing 5 mL of solution
139 (EM+DMSO or EM+drug). Embryos exposed to drugs or the sham control solution
140 were observed for morphological abnormalities every day until 5 dpf. Malformations

141 (e.g. spinal curvature, cardiac edema) were considered as experimental end-points
142 and when detected the corresponding animals were excluded from the study.

143 **Calcium imaging**

144 At 24hpf embryos of the (Hsp70:GAI4 x UAS:GCaMP6f;cry:mCherry) line were
145 exposed to a 38°C temperature for 1.5 hour. Upon heat shock activation, GCaMP6f is
146 expressed in all the cells of the animals.

147 At 2-3dpf the embryos were then individually embedded in low melting agarose, ventral
148 side up for imaging.

149 30 min time lapse series were acquired at 1 Hz, at a single focal plane, on an
150 Olympus BX60 microscope (Olympus corporation, Tokyo, Japan) equipped with a 40x
151 0.6N water immersion objective. A non-laser spinning disk system (DSD2, ANDOR
152 Technology, Oxford, UK) was used for illumination and image acquisition. Images were
153 open in Fiji and analyzed using Multi Measure (W. Rasband, B. Dougherty), Measure
154 Stack (Optinav, Redmond, WA), and custom Image J plugins. Regions of interest
155 (ROIs) were drawn manually over individual cell bodies. Movements of the
156 preparation in the X/Y axis were corrected using the plugin Measure Stack. Average
157 gray level from pixels in ROIs was measured over time. Spikes were defined as
158 increase of fluorescence higher than 2 times the standard deviation of the baseline.
159 The duration of spikes was calculated as the width at half-maximum. Incidence was
160 scored as the number of cells generating transients divided by the estimated total
161 number of cells in the imaged field and was expressed as a percentage. Frequency
162 was calculated as the total number of transients in a given cell divided by the total
163 acquisition time and was expressed as spikes per hour.

164 **Immunohistochemistry**

165 *Tissue preparations*

166 6-7 dpf zebrafish larvæ were deeply anesthetized using 0.2% Ethyl3-
167 amniobenzoate methanesulfonate (MS222; Sigma-Aldrich) diluted in EM, then they
168 were fixed in ice-cold 4% paraformaldehyde (PFA; Electron Microscopy Sciences) in
169 1X phosphate-buffered saline (PBS; Fisher Scientific) containing 0.1% Tween20
170 (PBST) overnight at 4 °C. Samples were dehydrated and stored in MeOH at -20°C.

171 *Immunofluorescence*

172 Immunofluorescence was performed in 2 mL microtubes. Unless specified
173 otherwise in the protocol, incubations were performed at Room Temperature (RT), and
174 thorough PBST washes were performed between each steps. The samples were first
175 incubated in 3% Hydrogen Peroxide Solution (H₂O₂) in Ethanol 100 (EtOH) for 30
176 minutes, to deactivate endogenous peroxidases. They were then successively
177 incubated in EtOH:Xylen 1:1 without agitation for 1 h and, at -20°C, in EtOH:Aceton 1:2
178 without agitation for 20 minutes. The washes were performed between these steps
179 were performed in EtOH. After the final wash, samples were rehydrated in PBST.

180 In order to unmask the antigens, samples were incubated in PBST:Tris 150 mM
181 pH9 for 10 minutes, then in Tris 150 mM pH9 at RT for 10 minutes and at 70°C for 30
182 minutes. After PBST washes, the samples were incubated in a blocking buffer (10%
183 normal goat serum (NGS), 1% triton X-100, 1% tween-20, 1% DMSO, 1% Bovin Serum
184 Albumin (BSA) in PBS 1X) for 3 hours.

185 Two protocols were used for primary antibody staining. For the TH antibody, the
186 samples were incubated with the first primary antibody (mouse anti-TH, 1:250) in a
187 staining solution (1% NGS, 1% triton X-100, 1% DMSO, 1% BSA, 0,05% azide sodium
188 in PBST) at 4°C for 7-10 days, under gentle agitation. The samples were then

189 incubated in a blocking buffer DAB (4% NGS, 0,3% triton X-100, 0,5% DMSO in PBST)
190 for 1 hour at RT and incubated with a first secondary antibody (anti-mouse biotinylated,
191 1:200) in a secondary staining buffer (4%NGS, 0,1% triton X-100 in PBST) for 2,5 days
192 at 4°C under gentle agitation.

193 For the revelation, we used the Vectastain ABC kit (Vector ®).Briefly, a AB mix
194 was prepare by adding 10µl of solution A and 10µl of solution B in 1mL PBST/1%
195 Triton-X100. One hour after the preparation, the samples were incubated in the AB mix
196 for 1 hour. Samples were then incubated in Tyramid-TAMRA (1:200 in PBST) for 20
197 minutes, then 0,012% H2O2 was added directly in the solution and the samples were
198 incubated for an additional 50 minutes.

199 Before a second primary antibody incubation, the samples underwent a step of fixation
200 in PFA 4% for 2 hours at RT and washed overnight in PBST.

201 For the other primary antibodies (rabbit anti-caspase3, 1:500 or chicken anti-GFP,
202 1:500), the samples were incubated in the blocking buffer (1h when following a TH
203 staining, 3h otherwise), then they were incubated with the primary antibody in a
204 staining solution at 4°C for 3-4 days, under gentle agitation. After washes, the samples
205 were incubated with the second secondary antibody (goat anti-chicken Alexa Fluor
206 488, 1:500) and DAPI 1X in PBST at 4°C for 2,5 days under gentle agitation. Samples
207 were then washed three times in PBST and left overnight in PBST. For observation,
208 the brain were dissected and mounted between slides and coverslides in Vectashield
209 solution (Vector®).

210 *Image acquisition*

211 A Leica TCS SP8 laser scanning confocal microscope with a Leica HCTL Apo
212 × 40/1.1 w objective was used to image the specimens.

213 Fluorescence signal was detected through laser excitation of fluorophores at 405, 488,
214 552, or 638 nm and detection was performed by two internal photomultipliers. Steps in
215 the Z-axis were fixed at 1 μm . Acquired images were adjusted for brightness and
216 contrast using ImageJ/FIJI software.

217 *Quantification of immuno-reactive cells*

218 The TH- and GFP-IR cells were counted manually from z-stacks of confocal
219 images using the ImageJ cell counter plugin.

220 **Spontaneous locomotion assays**

221 Individual larvæ were placed in a well of a 24 well plate with 2mL EM 2hrs before
222 recordings for habituation. The plate is then placed in a Zebrabox (Viewpoint, Lyon,
223 France) for 10 minutes recording sessions. Locomotor activity was recorded using
224 ZebraLab software (Videotrack; ViewPoint Life Sciences, France). After a first session
225 without threshold for 24 untreated larvæ the average speed (av_sp) of the batch was
226 extracted from the data. For subsequent sessions, two threshold were applied. Swim
227 bouts with a speed below half the average speed ($av_sp/2$) were considered as
228 inactivity, episodes with a speed over twice the average speed (av_sp*2) were
229 considered as fast episode or burst and episodes with a speed between the two
230 threshold were considered as cruises episodes or normal swim.

231 For each sessions, each animal and each category of episodes (inactivity, cruises
232 episodes and bursts episodes), 4 parameters are extracted from the recordings: the
233 number of episodes, the total distance covered, the duration of activity, and the
234 average speed.

235 **Experimental design**

236 **Statistical analyses**

237 Results are shown as means \pm SEM. Means comparisons were performed using
238 the appropriate non parametric statistical tests (ANVOA, Mann Whitney U test or
239 Kruskal-Wallis test depending on the experimental conditions). $P < 0.05$ was
240 considered statistically significant and noted as follow: $P < 0.05$ (*), $P < 0.01$ (**), $P <$
241 0.001 (***)).

242 For percentages, we used the 95% confidence interval defined as
243 $=1.96 \cdot \text{squareroot}((x \cdot (1-x)/n))$, n being the number of independent samples and x being
244 the % of change observed.

245 All statistical tests were performed using the online software Brightstat and R.

246 **Results**

247 **Presence of calcium spikes in the brain of zebrafish embryo.**

248 To study Embryonic Neuronal Excitability (ENE) in the embryonic zebrafish brain,
249 we recorded calcium spikes as a proxy. To follow the dynamics of intracellular calcium
250 concentration we used the (Hsp70:GAI4 x UAS:GCaMP6f;cry:mCherry) transgenic
251 line, in which the genetically encoded calcium reporter GCamp is expressed upon heat
252 shock activation (see Materials and Methods). To monitor changes in fluorescence
253 over time, we performed time-lapse imaging of the anterior most part of the brain of 2-
254 3dpf zebrafish embryos for 30 minutes sessions.

255 Spontaneous changes in fluorescence were detected in forebrain cells, likely
256 including presumptive dopaminergic cells in the telencephalon and the OB (Figure 1A).
257 We analyzed the evolution of the fluorescence from selected regions of interest
258 corresponding to individual cell bodies (Figure 1B and Materials and methods). The

259 average frequency of the recorded Ca^{2+} spikes was 6.6 ± 5.4 spikes.h⁻¹; the average
260 incidence of these events was $45.2 \pm 9.7\%$; these events had a mean duration of $3.3 \pm$
261 1.6 s (n= 28 spikes from 5 independent preparations Figure 1C, blue boxplots). These
262 parameters are in the range of what has been reported in the zebrafish spinal cord,
263 confirming that the duration of Ca^{2+} spikes is shorter in zebrafish than in xenopus
264 (Dulcis & Spitzer, 2008; Warp et al., 2012; Plazas et al., 2013).

265 **Global pharmacological modifications of calcium spikes dynamics**

266 In order to assess the effects of global manipulations of ENE, we applied
267 pharmacological compounds directly in the embryo medium. The treatments were
268 performed during the last day of embryonic development (48-72hpf) to reduce the
269 effects on early developmental steps such as neurulation and proliferation. These
270 drugs were already used in *Xenopus* for similar purposes (Borodinsky et al., 2004). To
271 increase calcium spiking we used veratridine (10 μM), which blocks the inactivation of
272 voltage-dependent sodium channels. To decrease calcium spiking, we used a cocktail
273 containing TTX (2 μM), ω -Conotoxin (0.08 μM), Nifedipine (0.4 μM) and Flunarizine (2
274 μM) targeting respectively voltage-dependent sodium channels; N, L and T subtypes
275 of voltage dependent calcium channels (we refer to this cocktail as TCNF based on
276 the initials of its 4 components).

277 We performed time-lapse recordings of the (Hsp70:GAI4 x
278 UAS:GCaMP6f;cry:mCherry) transgenic line two to ten hours after the beginning of the
279 treatments.

280 Following either veratridine treatment (n=26 spikes from 4 independent
281 preparations) or TCNF treatment (n=15 from 4 independent preparations), individual
282 events had a similar duration as in control (Kruskal-Wallis test, $p=0.538$; Figure 1C).
283 Following veratridine treatments, the average frequency of calcium spikes was

284 increased (+39.3 \pm 16%, n=36 cells from 4 independent preparations, p=0.206
285 bonferroni post-hoc test) as well as the average incidence of calcium transients
286 (29.9 \pm 45% n=4 independent preparations, p<0.05 conover posthoc comparisons;
287 Figure 1C, green boxplots).

288 Following TCNF treatments, the average frequency of calcium spikes was
289 decreased (-29 \pm 22%, n=17 cells from 4 independent preparations, p=0.812
290 bonferroni post-hoc test) as well as the average incidence (-44 \pm 48% n=4
291 independent preparations, p<0.01 Kruskal-Wallis paired comparisons)(Figure 1C, red
292 boxplots).

293 These results demonstrate that balneation treatments are able to change the
294 incidence and frequency of spontaneous calcium spikes in the embryonic zebrafish
295 forebrain. Based on these results, we refer to veratridine treatment as “increase of
296 ENE”, and to TCNF treatment as “decrease of ENE”, in the following sections of the
297 manuscript.

298 **Dopaminergic cells in the telencephalon and the olfactory bulb (OB) in the** 299 **zebrafish brain at larval stages.**

300 To identify dopaminergic neurons in the telencephalon and the OB, we used two
301 markers of the catecholaminergic phenotype, immune-labeled tyrosine hydroxylase 1
302 (TH1), the rate limiting enzyme for dopamine synthesis and the vesicular monoamines
303 transporter (vMAT2) combined to anatomical landmarks such as the position of brain
304 ventricles or large fibers bundles. Indeed, in zebrafish, like in mammals, noradrenaline-
305 containing neuronal soma are not detected in the forebrain anterior to the midbrain-
306 hindbrain boundary, rather, they are restricted to neuronal subpopulations located in
307 the nucleus locus coeruleus, the medulla oblongata and the area postrema (Ma,

308 1994a; b, 1997, 2003). Thus, all the catecholaminergic neurons located in front of the
309 midbrain-hindbrain boundary are likely to be dopamine neurons.

310 To localize these markers we performed double wholemount
311 immunohistochemistry on 6-7 dpf larvæ of the Tg(Et.vMAT2:eGFP) transgenic line.
312 We used an anti-GFP antibody to amplify the endogenous GFP signal to visualize cells
313 expressing vMAT2 (referred to as vMAT2+ cells in the remaining of the manuscript)
314 and an anti-TH antibody to identify TH1 cells (referred to as TH1+ cells in the remaining
315 of the manuscript). This anti-TH antibody is specific to TH1 and does not have affinity
316 for TH2 (Yamamoto et al., 2011).

317 In control conditions, in the telencephalon, we detected 15.1 ± 3.1 TH1+ cells (n=
318 39 samples from 6 independent experiments; Figure 2A, left column, Figure 2B, blue
319 boxplot). The cell bodies of these neurons were distributed bilaterally along the midline,
320 and relatively close to it. The major pattern of fibers distribution we could detect was
321 that of fibers projecting first ventrally and then laterally joining the wide dopaminergic
322 lateral longitudinal tracts.

323 An average of 63.4 ± 6.7 vMAT2+ cells was also detected in this region (n= 39
324 samples from 6 independent experiments; Figure 2A, blue boxed column, Figure 2 C
325 blue boxplot). The overall disposition of the cell bodies and projections was the same
326 as for TH+ cells.

327 In control conditions, in the OB, 46.4 ± 8.1 vMAT2+ cells and 30 ± 2.6 TH1+ cells
328 were detected (n= 39 samples from 6 independent experiments; Figure 2A, blue boxed
329 column and Figure 2D and 2E, blue boxplot). The cell bodies of these OB TH1+
330 neurons were distributed at the anterior end of the forebrain and they were initially
331 projecting in an anterior direction before rapidly branching in multiple directions.

332 In both regions, all TH1+ cells were also vMAT2+ while some vMAT2+ cells were
333 TH1-. In the telencephalon, vMAT2+/TH1- cell bodies were mostly located at the
334 anterior end of the cluster of vMAT2/TH1+ cells. Such vMAT2+/TH- cells are also
335 detected in the telencephalon of adult zebrafish (Yamamoto et al., 2011). Thus, in the
336 developing zebrafish telencephalon, the population of vMAT2+ cells slightly exceeds
337 that of TH1-expressing cells.

338 **Effects of pharmacological treatments on the expression of dopaminergic** 339 **markers in the telencephalon and the OB.**

340 To assess the effects of ENE on the expression of telencephalic dopaminergic
341 markers at larval stages, we applied pharmacological treatments by balneation from
342 48 to 72 hpf as described above and performed whole-mount immunohistochemistry
343 on larvæ fixed at 6-7 dpf.

344 Increasing the excitability in the zebrafish brain also increased the number of TH1+
345 cells both in the telencephalon and in the OB (+28.6+/-15%, $p < 0.05$ and +45.9+/-17%
346 $p < 0.001$ respectively, $n = 35$ samples from 6 independent experiments, conover
347 posthoc comparisons, Figure 2A, green boxed column; Figure 2B and 2D, green
348 boxplots). Meanwhile, the number of vMAT2 cells did not change significantly in either
349 regions ($p = 0.08$ for the telencephalon, $p = 0.659$ for the OB, Kruskal wallis test; $n = 16$
350 samples from 6 independent experiments; Figure 2A, green boxed column, Figure
351 2C,E, green boxplots).

352 Following decreased excitability, the number of TH1+ cells diminished in the
353 telencephalon but not in the OB (-14.5+/-9.6% and -0.7+/-7.3% respectively, $n = 49$
354 samples from 6 independent experiments; $p < 0.001$ and $p > 0.05$ respectively, conover
355 posthoc comparisons, Figure 2A, red boxed column, Figure 2B and 2D, red boxplot).
356 Meanwhile, the number of vMAT2 cells did not change significantly in either regions

357 (Kruskal wallis test: $p=0.08$ for the OB, $p=0.659$ for the OB; $n=24$ from 6 independent
358 experiments; Figure 2A, red boxed column and Figure 2C and 2E, red boxplots). In
359 both experimental situations, that is, after increasing or decreasing ENE, all the TH1+
360 cells also exhibited vMAT2 labelling. Hence, according to our identification criteria
361 (anatomical position combined to the expression of TH and vMAT2), an increase of
362 embryonic electrical activity increases the number of TeIDA cells, while a decrease of
363 embryonic electrical activity decreases the number of TeIDA cells.

364 On the other hand, the number of vMAT2+ cells was relatively stable in comparison
365 to TH1+ cells following the perturbation of activity (only decreasing in the telencephalon
366 following a decrease of activity). The stability of the number of vMAT2+ cells and the
367 lower proportion of vMAT2+/TH- cells following increase of ENE suggest that the cells
368 that express a complete dopaminergic phenotype in this condition are recruited among
369 a population of vMAT2+/TH-cells. Hence vMAT2+/TH-cells would behave as a reserve
370 pool for dopaminergic cells (Dulcis & Spitzer, 2012). A similar conclusion could also
371 apply to the OB, despite the fact that the number of TH1+ cells is not statistically
372 diminished following decreased activity in this region. This unexpected result could
373 account for a number of TH1+ cells already set at a minimum in basal conditions in the
374 OB.

375 **Modifications of ENE do not have an effect on cell death in the forebrain**

376 To check whether increase or decrease of ENE could change cell survival, we
377 counted the number of cells IR for the apoptosis marker caspase-3 at 6-7 dpf. The
378 number of caspase-3+ cells was stable following the increase or the decrease of ENE,
379 strengthening the hypothesis that the changes observed in the number of TH1+ cells
380 is indeed linked to changes in specification rather than changes in cell death (Figure
381 3).

382 **Maturation of spontaneous swimming in zebrafish larvæ**

383 In order to analyze the consequence of changes in ENE on motor behaviors in
384 zebrafish larvæ, we recorded swimming episodes, as described in Materials and
385 Methods. During locomotion, zebrafish larvæ display successive turn and swim bouts
386 called episodes, interleaved with resting periods. This behavior can be analyzed by
387 semi-automated methods, making possible to distinguish between episodes based on
388 the average swim speed. Swimming episodes with a speed close to the overall average
389 speed of all recorded episodes are considered as cruises episodes or normal swim.
390 Episodes with a speed higher than twice the overall average speed of all recorded
391 swim episodes, are considered as fast episodes or bursts.

392 We first studied the dynamic of maturation of larval cruises and bursts episodes in
393 control conditions. We tracked the position of individual larvæ during 3 rounds of 10
394 minutes recordings at 4, 5, 6 and 7 dpf. The recorded parameters reflected a gradual
395 increase of spontaneous locomotion from 4 to 6 dpf and a relative stability between 6
396 and 7dpf. From 4 to 6 dpf, the number of episodes, the duration of swimming and
397 distance covered increases, both for cruises and bursts episodes ($p < 0.01$ for each
398 parameters, Bonferroni post-hoc test, $n=48$ individuals for each stages; Figure 4,
399 lighter blue boxplots). In contrast, between 6 and 7 dpf, the recorded parameters were
400 stable both for cruises and bursts episodes ($p=0.16$, 1 and 1 respectively; Figure 4,
401 darker blue boxplots). Based on these results, we concluded that we could set our
402 analysis window between 6 and 7 dpf.

403 **Effects of pharmacological treatments on the locomotion of 6-7 dpf larvæ.**

404 We next studied the effect of transient increase and decrease of ENE during the
405 embryonic period on locomotion recorded in larval zebrafish (Figure 5A). We recorded
406 spontaneous locomotion of 6-7 dpf zebrafish larvæ over 3 consecutive 10 minutes

407 sessions in 3 conditions: control, increased ENE, and decreased ENE. A
408 representative example of traces obtained for 24 well plates for each conditions is
409 shown in Figure 5B. For cruises and bursts episodes, the four parameters measured
410 were the number of swim bouts, the total duration of swim, the total distance covered,
411 the average speed of swim (Figure 5 C-J).

412 For cruises episodes, in control conditions, the four measured parameters were
413 the number of swim bouts: 1267.2 ± 292.3 , total duration: 306.5 ± 58.6 s, total distance
414 covered: 767.5 ± 285.1 mm and average speed: 2.5 ± 0.7 mm.s⁻¹ (n=318 larvæ from
415 15 independent experiments, Figure 5B-F, blue boxplots).

416 The number of swim bouts was decreased following both the increase and the
417 decrease of ENE ($-5.8 \pm 2.3\%$; $-22 \pm 5\%$ respectively, Figure 5C). The three other
418 parameters increased either after an increase or a decrease of ENE (the total duration:
419 $+4.6 \pm 2.1\%$; $+35.4 \pm 5.8\%$; the total distance covered: $+38.3 \pm 4.9\%$; $+14.7 \pm 4.3\%$
420 and average speed: $+34.6 \pm 4.8\%$; $+22.2 \pm 5\%$ respectively, $p < 0.01$ conover posthoc
421 comparisons; n>262 larvæ from 15 independent experiments; Figure 5D-F).

422 For bursts episodes, in control conditions, the 4 parameters studied were the
423 number of swim bouts: 301 ± 227.6 , the total duration: 42 ± 38.4 s, the total distance
424 covered: 434.2 ± 492.6 mm and the average speed of swim: 9.7 ± 2.8 mm.s⁻¹ (Figure
425 5 G-J, blue boxplots).

426 Three of these parameters changed according to the treatments. They increased
427 following an increase of ENE and decreased following a decrease of ENE (number of
428 swim bouts: $+24.6 \pm 4\%$; $-54.8 \pm 6\%$; total duration: $+37.8 \pm 4.8\%$; $-58 \pm 6\%$; total
429 distance covered: $+58.8 \pm 5\%$; $-61.6 \pm 5.9\%$ respectively, % of change followed by the
430 confidence interval, n>262 larvæ from 15 independent experiments; $p < 0.01$ conover

431 posthoc comparisons, Figure 5G-J). Average speed also increased following a
432 increase of ENE (+17+/-3.8% Figure 5J, green boxplot) while it did not change
433 following a decrease of ENE (Figure 5J, red boxplot).

434 These results showed that the consequences of perturbing the embryonic
435 electrical excitability are different on the cruises episodes and on bursts episodes,
436 suggesting that the underlying neural networks of these swimming modes are not the
437 same and/or that they are not regulated in the same way following changes in ENE.

438 **Kinetics of the direct effects of acute pharmacological treatments on the** 439 **locomotion of 6-7 dpf larvæ.**

440 To exclude a direct effect of the drugs used on the larvæ locomotion, we next
441 followed the time course of the effects of acute pharmacological treatments (veratridine
442 and TCNF) in 6-7 dpf larvæ. We performed 10 minutes recording sessions before
443 application of the treatments, then +2hrs, and 24hrs after the treatments.

444 For cruises episodes, the results obtained following acute veratridine applications
445 are close from the one induced by the embryonic applications with a decrease of the
446 number of episodes and an increase of the duration and the distance. Only the results
447 for the average speed are different since it was not significantly different following acute
448 application while it increased following embryonic application (Figure 6A-D green
449 boxplots). Following T.C.N.F applications the number of events decreased like similarly
450 as following embryonic application while duration, distance and average speed
451 remained unchanged (Figure 6A-D red boxplots).

452 For bursts episodes, acute treatments had overall similar effects on the recorded
453 parameters as the one recorded after treatments performed in 2-3 dpf embryos (Figure
454 6). Veratridine application induced an increase of duration and distance, while the

455 number of events and the average speed were not significantly different (Figure 6E-H
456 green boxplots). T.C.N.F application led to a decrease of number of events, duration
457 and distance during bursts, only the average speed remained unchanged (Figure 6E-
458 H red boxplots).

459 By the next day, while some of the effects of the acute treatments are still
460 detectable, all the effects of these treatments on bursts episodes had faded away
461 (Figure 6E-H, lighter colored boxplots). These results clearly show that the delay
462 between the embryonic treatments and our analysis of larval locomotion is longer than
463 the time required for the disappearance of the acute effect of the drugs. Hence, these
464 results support the existence of a long-term effect related to changes in electrical
465 activity during the embryonic period in the zebrafish.

466 **Discussion (1257 / 3000w)**

467 *Summary*

468 Immature forms of excitability, referred to here as Embryonic Neuronal Excitability
469 (ENE), including calcium spikes and activation of non-synaptic receptors to
470 neurotransmitters, contribute to modulate neuronal differentiation. Here we show that
471 the developing zebrafish is a suitable model to manipulate ENE using pharmacological
472 treatments and to study the consequences of these manipulations on the plasticity of
473 neuromodulator systems, at works in the pathogenesis of several human
474 neuropsychiatric diseases. Indeed, we report that ENE exerts a positive regulatory
475 effect on the specification of the dopaminergic phenotype by increasing the number of
476 dopamine cells in the telencephalon. The pharmacological manipulation of ENE has
477 also a clear behavioral outcome by changing the occurrence of high-speed episodes
478 of swimming in zebrafish larvæ.

479 *Balneation treatments and ENE*

480 For the present study, zebrafish embryos were exposed to pharmacological
481 compounds by means of balneation treatments. This methodological approach allows
482 performing global and transient drugs applications, relevant to natural situations where
483 embryos can be exposed to various biologically active or toxic compounds. Zebrafish
484 is highly suitable for such questions because of its external development in an egg,
485 and because its blood brain barrier is not fully mature until 10 dpf, allowing diffusion of
486 the drugs to the neuronal tissues. As a consequence, we were able to analyze
487 alterations by pharmacological treatments of calcium transients, one of the main form
488 of immature excitability.

489 We focused on calcium transients to assess the effectiveness of the treatments, but
490 other intercellular communication processes such as the paracrine activation of GABA

491 and glutamate receptors by endogenous transmitters are also likely perturbed by the
492 treatments. Further studies are required to decipher the specific contribution of each
493 of these mechanisms to the cellular and behavioral effects we reported here.

494 *Calcium transients in the zebrafish forebrain*

495 One reason to focus on calcium transients is that they have been involved in
496 neurotransmitter phenotype specification in other models of neuronal plasticity. In
497 addition, calcium transients are conveniently measured by calcium imaging.

498 Calcium transients were already reported in the spinal cord of zebrafish embryos
499 around 24hpf. Here, recordings were performed in the forebrain of embryonic zebrafish
500 around 48hpf, a time at which the transition toward synaptic network activity has
501 occurred in the spinal cord. These observations are in accordance with the existence
502 of an postero-anterior gradient of neuronal maturation, similar to what was described
503 in xenopus.

504 Calcium transients in the forebrain had frequency and duration similar to what has
505 been described in the zebrafish spinal cord. This duration is overall shorter than what
506 has been observed in the *Xenopus* nervous system. The basis of these interspecies
507 differences are not known, but it suggests that the duration of the transients is not
508 necessarily the pertinent signal to trigger the effect on neuronal differentiation. This is
509 further suggested by the results of the TCNF treatments reported here, which lead to
510 changes in DA specification and in locomotion parameters, while the duration of
511 individual spikes duration was not changed.

512 We chose to drive the expression of GCamp by an exogenous trigger, here a heat-
513 shock. This allowed the expression of the calcium reporter in all the cells present at
514 the selected period of recordings. The next step of our approach will thus be to use
515 differentiation markers of the DA lineage to identify the differentiation status of the cells

516 where the Ca^{2+} spikes are detected, and also to see whether there are different
517 dynamics of the calcium transients between different subregions of interest in the
518 embryonic brain by using whole brain calcium imaging.

519 *Identification of a biomarker for DA reserve pool neurons?*

520 The effect of ENE perturbations on the DA phenotype analyzed by the number of
521 TH1+ cells was in agreement with the homeostatic rule described in xenopus. Indeed,
522 DA phenotype was enhanced by increased excitability, as expected from an overall
523 inhibitory neurotransmitter. The relative constancy of the number of vMAT2+ cells,
524 together with the absence of significant change in caspase 3-labelled cells upon
525 treatments, suggest that modulation of excitability did not affect cell death or
526 proliferation, but rather triggered a plasticity of the dopaminergic phenotype. This
527 plasticity of the DA phenotype is likely to occur within the pool of vMAT2+ cells, since
528 the number of VMAT2+/TH+ was increased with increased excitability, at the expense
529 of VMAT2+/TH- cells. Therefore, the VMAT2+/TH- cells would be a reserve pool of
530 cells primed to become dopamine neurons when plasticity-triggering events occur.
531 Although somewhat peculiar at first sight, the expression of the vesicular transporter
532 in a reserve pools of cells, might have a functional advantage in term of response to
533 plasticity-triggering events, limiting the number of factors to be changed for reaching a
534 fully functional dopamine phenotype.

535 *Behavioral consequences of ENE*

536 Perturbations of ENE had also behavioral consequences in zebrafish larvæ. For
537 bursts episodes, the initiation of movement is likely to be the prime parameter modified
538 following ENE perturbations. Interestingly, hyperlocomotion is an endophenotype
539 related to ADHD and schizophrenia in zebrafish (Blin et al., 2008; Lange et al., 2018).
540 Determining whether a direct activation of TeIDA cells could trigger an increase of

541 bursts episodes is an interesting perspective for the future, as seeing whether other
542 behaviors related to ADHD and schizophrenia such as prepulse inhibition are also
543 affected by alterations of ENE.

544 *Critical period for the effect of ENE perturbations*

545 We observed an effect of the pharmacological treatments performed during the
546 embryonic period on spontaneous locomotion several days after the end of the
547 treatments. In contrast, no effects were observed 24h after treatments performed at
548 6dpf in the zebrafish larvæ. These long-lasting effects of treatments at specific
549 embryonic time are in line with the existence of a critical developmental period, more
550 sensitive to homeostatic perturbations, promoting therefore significant phenotypic
551 plasticity in immature neurons. Interestingly, dopaminergic systems have multiple
552 functional role and are particularly prone to plasticity events, suggesting that these
553 systems might be a key factor for adaptability of the animals to environmental changes.
554 Whether it is a cause, a consequence or a simple correlation of their conservation
555 throughout animal evolution is still an open question.

556 *Potential involvement of changes of ENE in the pathogenesis of brain disease*

557 According to the 'Developmental Origins of Health and Disease (DOHaD)
558 hypothesis, transient exposure to perturbations during the development could lead to
559 emergence of disease in young or adult individuals (Mandy & Nyirenda, 2018).
560 Neurological and psychiatric diseases, such as autism spectrum disorders, ADHD, or
561 schizophrenia are hypothesized to have a developmental origin. The environmental
562 factors potentially contributing to these pathologies include malnutrition, stress, and
563 drugs exposure during the embryonic period.

564 Results from epidemiological studies and experiments in rodents further suggest
565 that a range of functional and behavioral abnormalities observed in the mature system

566 result from early alterations of dopaminergic neurons differentiation. The data
567 presented here point to an implication of ENE in the regulation of dopaminergic
568 differentiation in the developing brain, suggesting that ENE could act as an
569 intermediate between environmental factors and the molecular changes leading to the
570 alteration of dopamine-related behaviors.

571 These results provide a firm basis to dissect further the cellular and molecular
572 mechanisms linking exposure to external challenges with the subsequent changes in
573 ENE, in the maturation of the dopaminergic systems and its behavioral outputs. A
574 comparative study of the transcription factors differentially expressed in vMAT2 cells
575 following changes in ENE, would help identify dopaminergic related factors having an
576 activity-dependent expression, including epigenetic effectors (level of methylation,
577 histone acetylation).

578 Such mechanisms are underlying phenotypes related to ADHD and schizophrenia
579 in zebrafish, and opens new avenues to better understand how environmental factors
580 could promote developmental brain disorders such as schizophrenia and ADHD.

581 **Bibliography**

582 Blankenship AG & Feller MB (2010) Mechanisms underlying spontaneous patterned
583 activity in developing neural circuits. *Nat.Rev.Neurosci.* 11:18–29.

584 Blin M, Norton W, Bally-Cuif L, Vernier P, Laure B-C & Vernier P (2008) NR4A2
585 controls the differentiation of selective dopaminergic nuclei in the zebrafish brain.
586 *Molecular and cellular neurosciences* 39:592–604.

587 Borodinsky LN, Root CM, Cronin JA, Sann SB, Gu X & Spitzer NC (2004) Activity-
588 dependent homeostatic specification of transmitter expression in embryonic
589 neurons. *Nature* 429:523–530.

- 590 Crepel V, Aronov D, Jorquera I, Represa A, Ben-Ari Y & Cossart R (2007) A
591 parturition-associated nonsynaptic coherent activity pattern in the developing
592 hippocampus. *Neuron* 54:105–120.
- 593 Demarque M, Represa A, Becq H, Khalilov I, Ben-Ari Y & Aniksztejn L (2002)
594 Paracrine intercellular communication by a Ca²⁺- and SNARE-independent
595 release of GABA and glutamate prior to synapse formation. *Neuron* 36:1051–
596 1061.
- 597 Demarque M & Spitzer NC (2010) Activity-Dependent Expression of Lmx1b
598 Regulates Specification of Serotonergic Neurons Modulating Swimming
599 Behavior. *Neuron* 67:321–334.
- 600 Dulcis D, Jamshidi P, Leutgeb S & Spitzer NC (2013) Neurotransmitter switching in
601 the adult brain regulates behavior. *Science* 340:449–453.
- 602 Dulcis D, Lippi G, Stark CJ, Do LH, Berg DK & Spitzer NC (2017) Neurotransmitter
603 Switching Regulated by miRNAs Controls Changes in Social Preference. *Neuron*
604 95:1319-1333.e5.
- 605 Dulcis D & Spitzer NC (2008) Illumination controls differentiation of dopamine
606 neurons regulating behaviour. *Nature* 456:195–201.
- 607 Dulcis D & Spitzer NC (2012) Reserve pool neuron transmitter respecification: Novel
608 neuroplasticity. *Developmental Neurobiology* 72:465–474.
- 609 Gawel K, Banono NS, Michalak A & Esguerra C V. (2019) A critical review of
610 zebrafish schizophrenia models: Time for validation? *Neuroscience and*
611 *Biobehavioral Reviews* 107:6–22.
- 612 Gomez TM, Robles E, Poo M & Spitzer NC (2001) Filopodial calcium transients

- 613 promote substrate-dependent growth cone turning. *Science* 291:1983–1987.
- 614 Gomez TM & Spitzer NC (1999) In vivo regulation of axon extension and pathfinding
615 by growth-cone calcium transients. *Nature* 397:350–355.
- 616 Klein MO, Battagello DS, Cardoso AR, Hauser DN, Bittencourt JC & Correa RG
617 (2019) Dopamine: Functions, Signaling, and Association with Neurological
618 Diseases. *Cellular and Molecular Neurobiology* 39:31–59.
- 619 Lange M, Froc C, Grunwald H, Norton WHJ & Bally-Cuif L (2018) Pharmacological
620 analysis of zebrafish *lphn3.1* morphant larvae suggests that saturated
621 dopaminergic signaling could underlie the ADHD-like locomotor hyperactivity.
622 *Progress in Neuro-Psychopharmacology and Biological Psychiatry* 84:181–189.
- 623 Lange M, Norton W, Coolen M, Chaminade M, Merker S, Proft F, Schmitt A, Vernier
624 P, Lesch K-P & Bally-Cuif L (2012) The ADHD-linked gene *Lphn3.1* controls
625 locomotor activity and impulsivity in zebrafish. *Molecular psychiatry* 17:855.
- 626 Ma PM (1994a) Catecholaminergic systems in the zebrafish. I. Number, morphology,
627 and histochemical characteristics of neurons in the locus coeruleus. *Journal of*
628 *Comparative Neurology* 344:242–255.
- 629 Ma PM (1994b) Catecholaminergic systems in the zebrafish. II. Projection pathways
630 and pattern of termination of the locus coeruleus. *Journal of Comparative*
631 *Neurology* 344:256–269.
- 632 Ma PM (1997) Catecholaminergic systems in the zebrafish. III. Organization and
633 projection pattern of medullary dopaminergic and noradrenergic neurons.
634 *Journal of Comparative Neurology* 381:411–427.
- 635 Ma PM (2003) Catecholaminergic systems in the zebrafish. IV. Organization and

- 636 projection pattern of dopaminergic neurons in the diencephalon. *Journal of*
637 *Comparative Neurology* 460:13–37.
- 638 Mandy M & Nyirenda M (2018) Developmental Origins of Health and Disease: the
639 relevance to developing nations. *International health* 10:66–70.
- 640 Murray RM, Bhavsar V, Tripoli G & Howes O (2017) 30 Years on: How the
641 Neurodevelopmental Hypothesis of Schizophrenia Morphed Into the
642 Developmental Risk Factor Model of Psychosis. *Schizophrenia Bulletin* 43:1190–
643 1196.
- 644 Owens DF & Kriegstein AR (1998) Patterns of intracellular calcium fluctuation in
645 precursor cells of the neocortical ventricular zone. *Journal of Neuroscience*
646 18:5374–5388.
- 647 Owens DF & Kriegstein AR (2002) Is there more to GABA than synaptic inhibition?
648 *Nat.Rev.Neurosci.* 3:715–727.
- 649 Plazas P V, Nicol N & Spitzer NC (2013) Activity-dependent competition regulates
650 motor neuron axon pathfinding via PlexinA3. *Proceedings of the National*
651 *Academy of Sciences of the United States of America* 110:1524–1529.
- 652 Scain AL, Le Corrionc H, Allain AE, Muller E, Rigo JM, Meyrand P, Branchereau P &
653 Legendre P (2010) Glycine release from radial cells modulates the spontaneous
654 activity and its propagation during early spinal cord development. *Journal of*
655 *Neuroscience* 30:390–403.
- 656 Schweitzer J & Driever W (2009) Development of the dopamine systems in zebrafish.
657 *Adv Exp Med Biol* 651:1–14.
- 658 Schweitzer J, Löhr H, Filippi A & Driever W (2012) Dopaminergic and noradrenergic

659 circuit development in zebrafish. *Developmental Neurobiology* 72:256–268.

660 Spitzer NC, Kingston PA, Manning TJ & Conklin MW (2002) Outside and in:

661 development of neuronal excitability. *Curr.Opin.Neurobiol.* 12:315–323.

662 Tay TL, Ronneberger O, Ryu S, Nitschke R & Driever W (2011) Comprehensive

663 catecholaminergic projectome analysis reveals single-neuron integration of

664 zebrafish ascending and descending dopaminergic systems. *Nature*

665 *Communications* 2:112–171.

666 Warp E, Agarwal G, Wyart C, Friedmann D, Oldfield CS, Conner A, Del Bene F,

667 Arrenberg AB, Baier H, Isacoff EY, Bene F, Arrenberg AB, Baier H & Isacoff EY

668 (2012) Emergence of patterned activity in the developing zebrafish spinal cord.

669 *Current Biology* 22:93–102.

670 Yamamoto K, Ruuskanen JO, Wullimann MF & Vernier P (2011) Differential

671 expression of dopaminergic cell markers in the adult zebrafish forebrain. *The*

672 *Journal of comparative neurology* 519:576–598.

673

674 **Author contributions:**

675 Ingrid Colin: Performed research, Analyzed data; Sandrine Bataille: Performed

676 research, Analyzed data; Hadrien Jalaber: Performed research, Analyzed data;

677 Damien Remy: Performed research, Analyzed data; Cynthia Froc: Performed

678 research, Analyzed data; Philippe Vernier: Designed research and Michaël Demarque:

679 Designed research, Performed research, Analyzed data, Wrote the paper.

Figure legends

Figure 1 Presence of calcium spikes in the zebrafish telencephalon and their manipulations by transient balneation in pharmacological agents.

A. Consecutive images of a confocal time series of the brain of 48 hpf of Et(hsp:gal4;UAS:GCamp6f) embryos in control conditions. Fluorescence is displayed on a pseudocolor scale, the look up images intensity scale coding is shown in the right corner of the first image. Scale bar is 100 μ m. White dash circle surround the cell body of a cell displaying a calcium transient.

B. Changes in fluorescence intensity are plotted as a function of time. Ca²⁺ transients were scored for fluorescence changes, more than two times the SD of the baseline (dashed lines), and >3 sec in duration, calculated as the width at half-maximum. Representative traces from control conditions (in blue), following veratridine treatment (in green) and following treatment with a pharmacological cocktail containing TTX (2.5 μ M), ω -Conotoxin (0.1 μ M), Nifedipine (0.5 μ M) and Flunarizine (2.5 μ M) (TCNF, in red).

C. Left, boxplots showing the mean duration of single calcium spikes in control conditions (in blue, 3.3 \pm 1.6 sec), following veratridine treatment (in green, 3.7 \pm 1.7 sec) and following TCNF treatment (in red, 3.4 \pm 1.4 sec).

Middle, boxplots showing the mean frequency of calcium transients in control conditions (in blue, 6.6 \pm 5.4 spikes per hour, n=28 cells from 5 independent preparations), following veratridine treatment (in green, 9.2 \pm 6.6 spikes per hour, n=36 cells from 4 independent preparations) and following TCNF treatment (in red, 4.7 \pm 3 spikes per hour, n=17 cells from 4 independent preparations).

Right, boxplots showing the mean incidence of single calcium spikes in control conditions (in blue, $45.2 \pm 9.7\%$, $n=5$ independent preparations), following veratridine treatment (in green, $58.8 \pm 9.7\%$, $n=4$ independent preparations) and in the presence of TCNF (in red, 4.7 ± 3 spikes per hour, $n=17$ cells from 4 independent preparations).

Figure 2 Effects of 24hrs balneation treatment on the number of dopaminergic neurons in the zebrafish larval telencephalon and OB.

A. Maximum projection of confocal z series of the brain of 6-7 dpf Et(VMAT2:eGFP) larvæ, in control conditions (left column boxed in blue), in the presence of veratridine (middle column, boxed in green) and in the presence of TCNF (right column, boxed in red). Immunostaining to TH (magenta) and GFP (cyan) and DAPI (yellow) are shown as merge and individual channels. Scale bars = 50 μm .

B-E. Boxplots showing the mean number of IR cells in control conditions, in the presence of veratridine and in the presence of “TCNF” in the telencephalon (B,C) and in the olfactory bulb (C,D), for TH (B,D) and for GFP (vMAT2 cells, C,E).

Figure 3 Absence of changes in cell death following increase or decrease of ENE

A. Maximum projection of confocal z series of the brain of 6-7 dpf Et(VMAT2:eGFP) larvæ, in control conditions (left image boxed in blue), in the presence of veratridine (middle image, boxed in green) and in the presence of TCNF (right image, boxed in red). Immunostaining to caspase-3 (magenta) and GFP (cyan) are shown as merged channels. Scale bars = 50 μm .

B. Boxplots showing the mean number of IR cells in control conditions, in the presence of veratridine and in the presence of “TCNF” for the caspase-3 staining in the olfactory bulb and the telencephalon.

Figure 4 Maturation of locomotion parameters

A-H. Boxplots showing the mean of 4 swimming parameters, number of episode (A,E), total duration (B,F), distance covered during swimming (C,G) and speed (D,H) for cruises episodes (A-D) and for bursts episodes (E-H) at different stage of larval development (4, 5, 6, and 7dpf).

Figure 5 Effects of 24hrs balneation treatments during embryonic development on spontaneous swimming of zebrafish larvæ.

A. Time line of the experiments indicating the timing (in days post fertilization, dpf) for the pharmacological treatments, and the following locomotion tests.

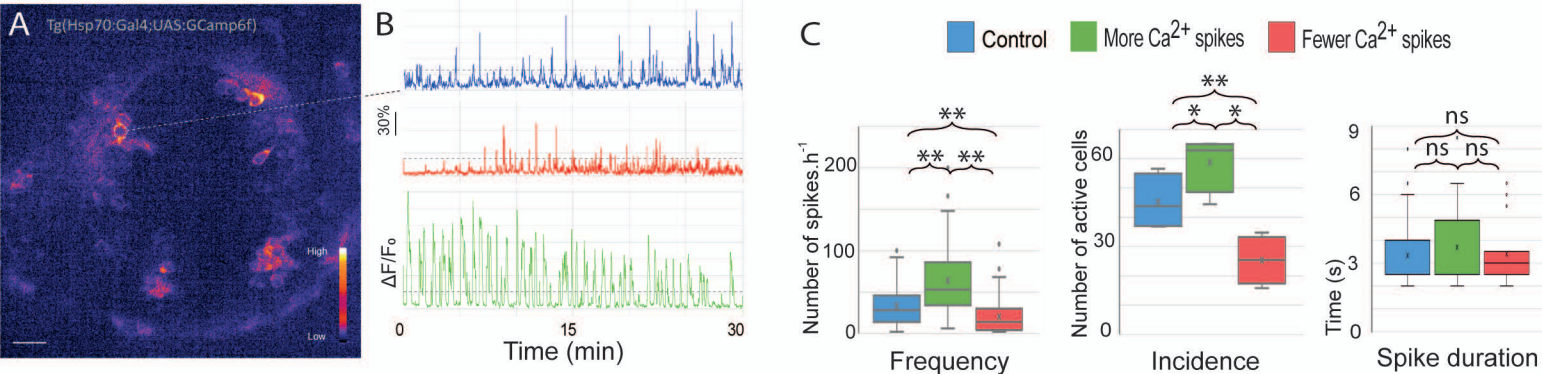
B. Representative path reconstructions for 24 individual larvæ during a 10 minutes trial for three experimental conditions. The portion of the path corresponding to bursts episodes (shown in red) are longer when early activity is increased (veratridine treatment) and shorter when early activity is decreased (T.C.N.F. treatment).

C-J. Boxplots showing the mean of different swimming parameters in different experimental conditions, Mean number of episode (C,G), total duration (D,H), distance covered during swimming (E,I) and speed (F,J) are shown for cruises episodes (C-F) and for bursts episodes (G-J).

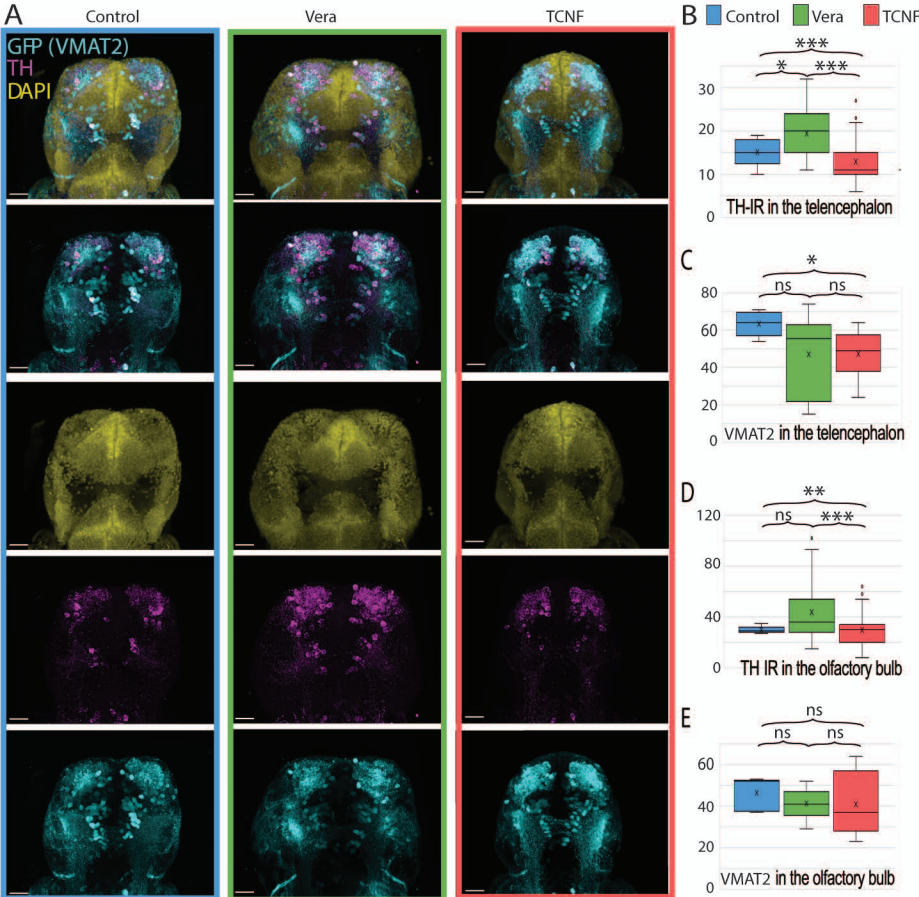
Figure 6 Effects of 2hrs acute balneation treatments on zebrafish spontaneous swimming.

A-H. Boxplots showing the mean of different swimming parameters, mean number of episode (A,E), total duration (B,F), distance covered during swimming (C,G) and speed (D,H), for cruises episodes (A-D) and for bursts episodes (E-H), in different experimental conditions. The effects of 2hrs acute treatments with DMSO,

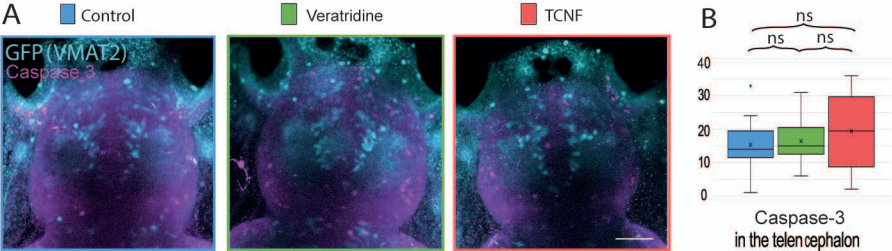
Veratridine, or TCNF are compared to pre-application recordings and 24hrs post-application recordings.



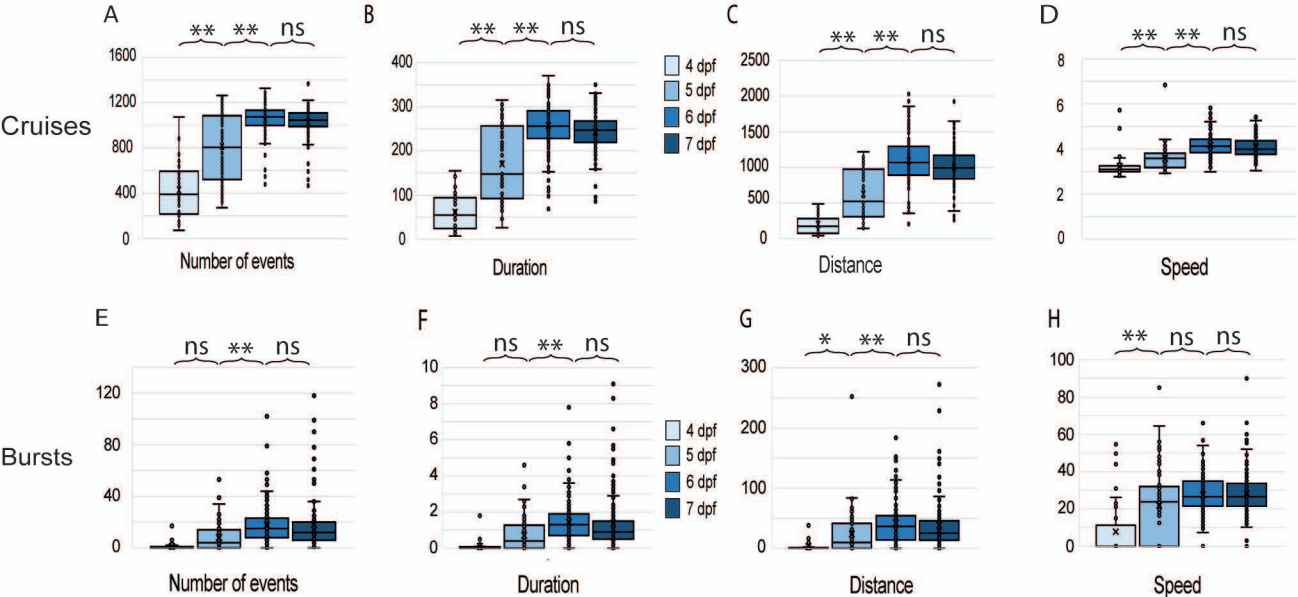
Bataille et al., Figure 1. Calcium spikes and their modulation by pharmacological treatments, in the embryonic zebrafish forebrain



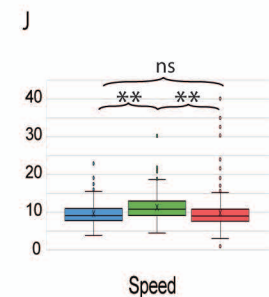
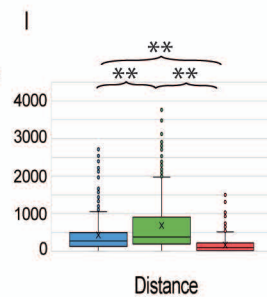
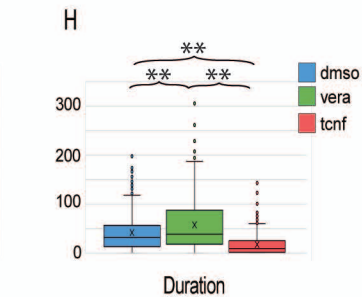
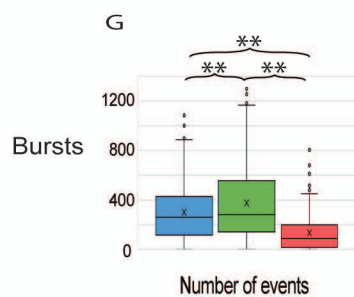
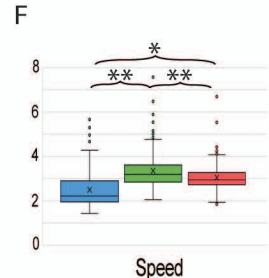
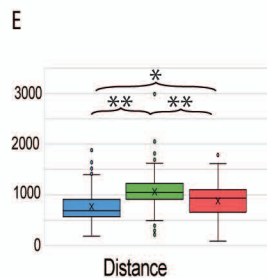
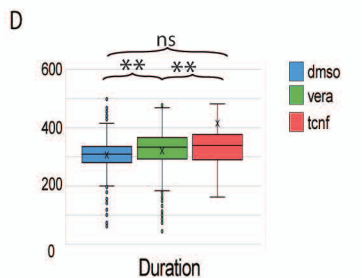
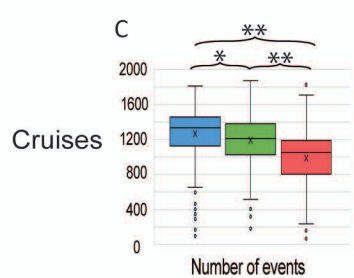
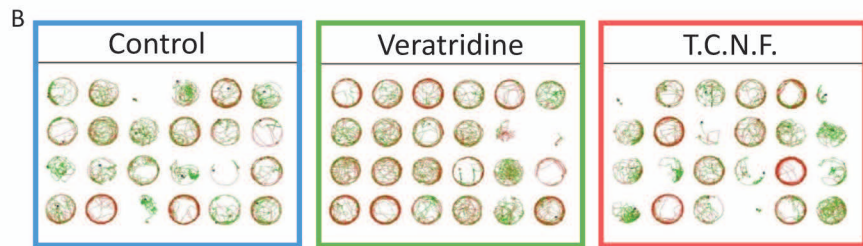
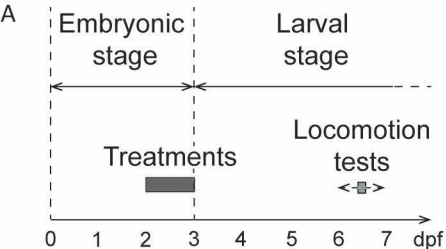
Bataille et al., Figure 2. Effects of ENE on the number of DA neurons in the zebrafish forebrain



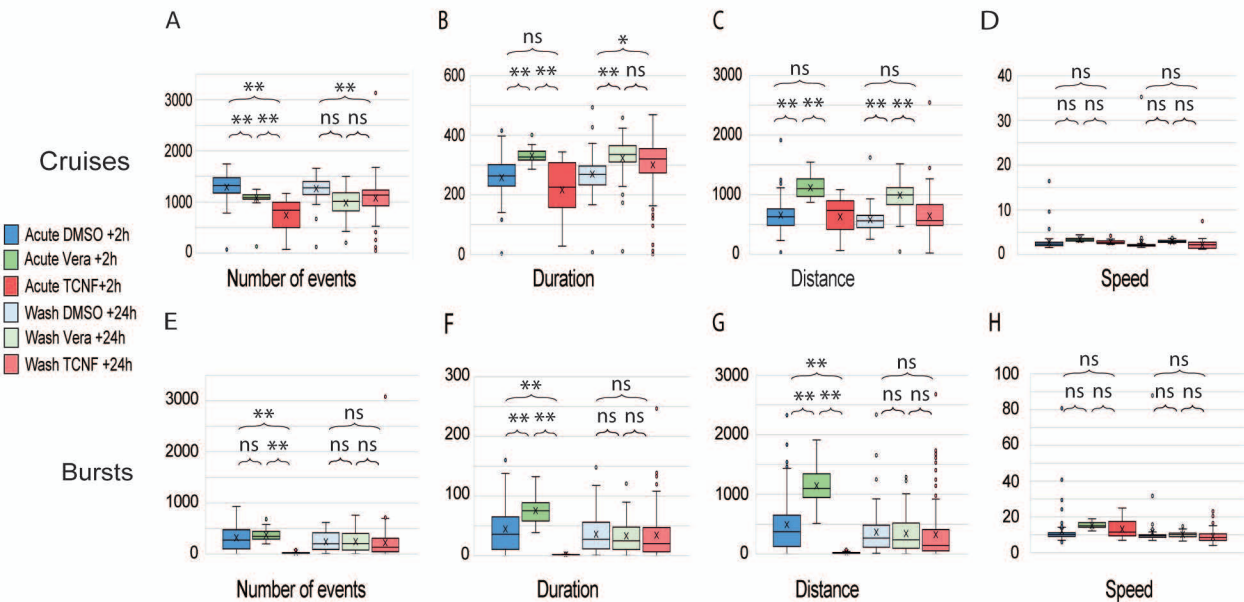
Bataille et al., Figure 3. Effects of ENE on caspase-3 expression in the larval zebrafish forebrain



Bataille et al., Figure 4. Development of zebrafish spontaneous locomotion



Bataille et al., Figure 5. Effects of ENE on the zebrafish spontaneous locomotion



Bataille et al., Figure 6. Effects of acute pharmacological treatments on the zebrafish spontaneous locomotion